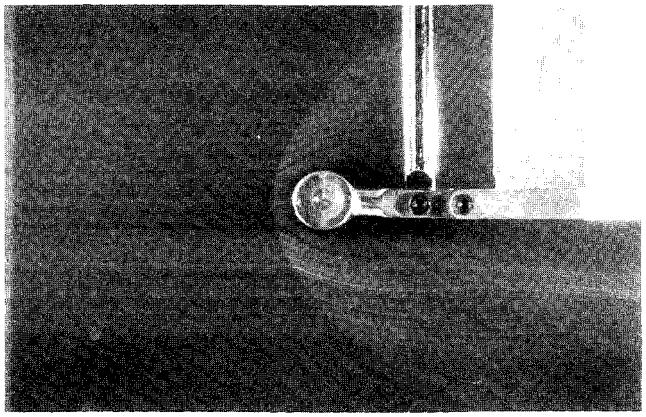

Fig. 2 Double-wedge airfoil at Mach 2.

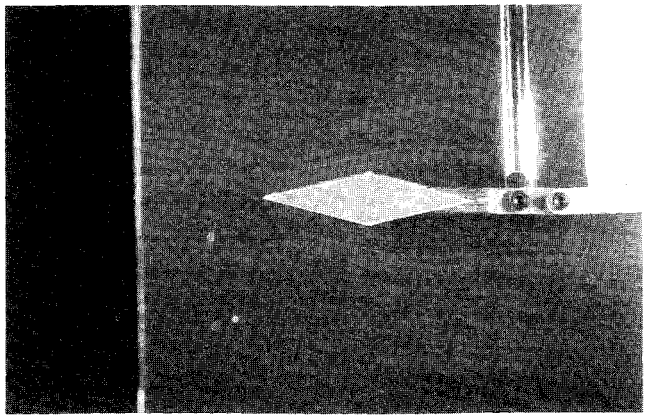

Fig. 3 Circular cylinder at Mach 2.

Two flash units were used to illuminate the smoke flow during tests. Each unit was positioned on the opposite side of the test section from the camera, approximately 60 deg off axis from the viewing direction. This orientation takes advantage of the good light-scattering character of smoke particles in the forward direction. The wind-tunnel window immediately opposite the model was painted black to provide a high-contrast image background. The tunnel windows, on the camera side, upstream and downstream of the model were also painted black to prevent direct viewing of the flash units by the camera. To minimize flash duration and to assure that the smoke motion was "frozen" during photography, each unit's power output was set at the lowest level. This power setting also results in a shorter recharge time allowing rapid photography at rates up to 3 frames/s.

Conducting flow-visualization experiments using this new method is relatively simple. Oil is dripped along the smoke-generation wire, current is applied, and then the tunnel is turned on. Once smoke filaments are produced the camera is activated taking typically 3–5 photographs. A minimal amount of synchronization between each step is necessary since the smoke-generation time is quite reasonable.

Results

The flowfield about a number of models was examined using the new smoke-visualization technique. For reasons of brevity, only the results for two models will be discussed. Each model was installed on a sting mount that was supported by a fairing and a strut allowing angle-of-attack adjustments.

Figures 2 and 3 show the smoke flow about a double-wedge airfoil and a circular cylinder, respectively. The flow is moving from left to right about the models, which have a maximum thickness of 1.12 cm and a span of 5.08 cm. As can be seen, there are a large number of approaching smoke filaments and the spacing is nearly uniform. The oblique shock extending from the airfoil leading edge and the detached shock in front of the cylinder are clearly indicated by abrupt bending of the smoke filaments. Expansion regions, around the models, are indicated by slowly bending or curving filaments. A shock wave produced by the angle-of-attack strut is observed in the area above and behind each model. It is important to emphasize that these images were obtained using only smoke; no schlieren or shadowgraph techniques were employed. The presence of shock waves and expansion regions is indicated strictly by changes in smoke-particle paths.

Smoke filament behavior in expansion regions, next to the models, was difficult to identify under some circumstances. One potential reason for this is that the smoke density is simply reduced as a result of the expansion, making filament visibility difficult. Another possible explanation could be related to the smoke particles' ability to "follow the flow" as affected by aerodynamic and inertial forces. No attempt was made, in this investigation, to assess possible particle inertial effects. The exact particle size and mass distributions are not known and were not measured. Despite this question, the visual quality and usefulness of the results seem worthy of value.

Conclusions

A number of conclusions are offered relative to the new smoke-visualization method developed.

1) The new visualization technique is very simple to implement on open-inlet induction type supersonic wind tunnels and has been demonstrated to be extremely effective. The smoke-generation and photography equipment employed is simple, inexpensive, and commonly available.

2) A large number of uniformly distributed and stable smoke filaments are produced. Shock waves and expansion regions are clearly identified by the smoke filament behavior.

3) The visualization accuracy may be affected by particle inertia effects. No attempt to address this possibility was undertaken.

4) Potential applications of this new smoke-generation technique to induction type wind tunnels operating at lower speeds exist.

References

[1]Mueller, T. J., "Flow Visualization by Direct Injection," *Fluid Mechanics Measurements*, edited by R. J. Goldstein, Hemisphere, New York, 1983, pp. 307–375.

[2]Mueller, T. J., "Smoke Visualization of Subsonic and Supersonic Flows (The Legacy of F.N.M. Brown)," Air Force Office of Scientific Research, AFOSR TR-78-1262, June 1978.

[3]Batill, S. M., and Mueller, T. J., "Visualization in the Flow Over an Airfoil Using the Smoke-Wire Method," *AIAA Journal*, Vol. 19, No. 3, 1981, pp. 340–345.

Importance of Fresh Air in Manometer Tubing

John M. Cimbala,* Richard S. Meyer,† and Todd B. Harman‡
Pennsylvania State University, University Park, Pennsylvania 16802

Introduction

IT has been found that poor quality air inside manometer tubing can lead to significant errors when measuring very

Received March 25, 1991; revision received April 11, 1991; accepted for publication April 26, 1991.

*Associate Professor, Department of Mechanical Engineering. Member AIAA.

†Research Assistant, Applied Research Laboratory, Department of Mechanical Engineering.

‡Graduate Assistant, Department of Mechanical Engineering. Member AIAA.

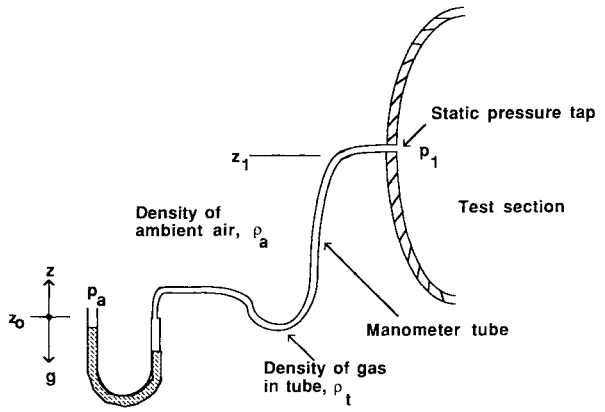

Fig. 1 Schematic diagram of typical pressure measurement setup.

low pressure differences, such as in a low-speed wind tunnel. A schematic diagram of a typical static pressure measurement setup is shown in Fig. 1. An electronic pressure transducer (or micromanometer) is often placed on a table at some elevation z_0, and the pressure tap is located at a different elevation z_1. The usual assumption is that the density ρ_t of the air inside the manometer tubing is the same as that of the ambient air ρ_a. In such a case, elevation difference $z_1 - z_0$ is irrelevant since the hydrostatic pressure rise in the atmosphere from z_1 to z_0 is identical to that in the tubing.

Observations

In our laboratory, while preparing for some high-accuracy pressure measurements with a setup similar to that of Fig. 1, it was discovered that the transducer zero was quite sensitive to elevation difference $z_1 - z_0$, contrary to intuition. Further investigation revealed that the air trapped inside the tubing was *denser* than the ambient air ($\rho_t > \rho_a$). Our analysis indicated a relative density difference of $(\rho_t - \rho_a)/\rho_a \approx 0.25$. In other words, the density of the gas inside the tubing was, in our test case, 25% larger than that of the ambient air! For a typical laboratory elevation difference of around 1 m, the corresponding pressure measurement error would be approximately 3.1 Pa (0.00045 psi, 0.012 in. of water.) Although this may at first appear negligible, note that the difference between stagnation and static pressure for the flow of air at 2.0 m/s is only about 2.4 Pa. The error due to the denser air in the tubing is certainly not negligible for low-speed flow measurements! Even at 10 m/s, if one tube from a pitot-static probe contained air at normal density, and the other tube contained air that was 25% more dense, the velocity reading from a transducer 1 m below the test section would read 10.25 m/s, an error of 2.5%.

Discussion

The obvious question is, How could the air inside the manometer tubing be so much denser than ambient air? The tubing used in our experiment was brand new, straight from its reel. Apparently, since the tubing is wound up like a garden hose immediately after it is manufactured, the gas inside the tubing would have virtually no chance to escape since the time of manufacture. The large observed density difference may be due to a number of factors, including outgassing of the plastic inside the tube or remnant gas from the manufacturing process. The authors have not analyzed the chemical composition of the gas trapped inside the manometer tubing. However, discussions with the manufacturer of the tubing (Hygenic Corporation of Ohio) verified our speculation that many types of plastic tubing are never blown out and may contain trapped gases such as water vapor and hydrocarbons. The concentrations of these gases are apparently high enough to increase the density of the air by about 25%.

In our laboratory, the situation was remedied by blowing out each section of manometer tubing with a small hand pump. The dense gas in the manometer tubing was thus replaced by fresh air, and the errors were completely eliminated. This is recommended by the authors as a preventative step prior to any pressure measurements, whenever new manometer tubing is being used.

Analytical Evaluation of Lattice Space Structures for Accuracy

Hiroshi Furuya*
Nagoya University, Chikusa, Nagoya 464-01, Japan

Introduction

EVALUATION of space structures has been performed conventionally in terms of structural strength, stiffness, vibrational characteristics, and controllability. However, the accuracy requirements for future large lattice space structures may require active control or static adjustment of the deformation. For example, a reflector support structure of a large space antenna will require extremely high accuracy to comply with electromagnetic requirements, the adaptive structures[1] need to be estimated for structural accuracy in order to design their controller systems, and a statically determinate structure also has an advantage of being free from thermal stresses.[2,3] To estimate the effects of random member length errors on the structural accuracy, some studies were reported earlier that were based on the approximate continuum analysis of the structures[4] and on multiple deterministic structural analyses of the truss (the Monte Carlo method) using the finite element analysis.[5]

The purpose of this study is to formulate the arbitrary stochastic effects of member length errors on the structural accuracy analytically. The comprehensive formulation presented here is based on vector subspaces associated with the dominant matrix, which is derived from the equilibrium matrix and the covariance matrix of the given structure, and it is shown that the stochastic analysis of the lattice-type structures can be treated as a simple eigenvalue problem, and that the invariant of the dominant matrix plays an important role in estimating the structural errors.

Effects of Random Member Length Errors

The errors induced in the lattice structures can be broadly divided into two types: stochastic and deterministic. The stochastic error is induced mainly due to member length tolerances, thermal expansions, and mission environment, whereas the deterministic error is mainly due to the nonlinearity of the various joints and the joint offsets. The present analysis regards that the errors can be represented by member length tolerances. Thus, this Note concentrates on the situation in which the nodal displacements are caused by errors in the lengths of the lattice members.

A three-dimensional lattice structure is defined as an assembly of straight members jointed at various nodal points. The relationship between the member length and the nodal position can be written as follows:

$$l_i^2 = (x_{i_1} - x_{i_2})^2 + (y_{i_1} - y_{i_2})^2 + (z_{i_1} - z_{i_2})^2 \qquad (1)$$

Received Aug. 15, 1990; revision received April 3, 1991; accepted for publication April 5, 1991.

*Assistant Professor, Structures Engineering, Department of Aeronautical Engineering.